Vol. 54, No. 6

Cellular Pharmacokinetics of the Novel Biaryloxazolidinone Radezolid in Phagocytic Cells: Studies with Macrophages and Polymorphonuclear Neutrophils[∇]

Sandrine Lemaire, Paul M. Tulkens, and Françoise Van Bambeke*

*Unité de Pharmacologie cellulaire et moléculaire and Louvain Drug Research Institute,
Université catholique de Louvain, Brussels, Belgium*

Radezolid (RX-1741) is the first biaryloxazolidinone in clinical development. It shows improved activity, including against linezolid-resistant strains. Radezolid differs from linezolid by the presence of a biaryl spacer and of a heteroaryl side chain, which increases the ionization and hydrophilicity of the molecule at physiological pH and confers to it a dibasic character. The aim of this study was to determine the accumulation and subcellular distribution of radezolid in phagocytic cells and to decipher the underlying mechanisms. In THP-1 human macrophages, J774 mouse macrophages, and human polymorphonuclear neutrophils, radezolid accumulated rapidly and reversibly (half-lives of approximately 6 min and 9 min for uptake and efflux, respectively) to reach, at equilibrium, a cellular concentration 11-fold higher than the extracellular one. This process was concentration and energy independent but pH dependent (accumulation was reduced to 20 to 30% of control values for cells in medium at a pH of <6 or in the presence of monensin, which collapses pH gradients between the extracellular and intracellular compartments). The accumulation at equilibrium was not affected by efflux pump inhibitors (verapamil and gemfibrozil) and was markedly reduced at 4°C but was further increased in medium with low serum content. Subcellular fractionation studies demonstrated a dual subcellular distribution for radezolid, with ~60% of the drug colocalizing to the cytosol and ~40% to the lysosomes, with no specific association with mitochondria. These observations are compatible with a mechanism of transmembrane diffusion of the free fraction and partial segregation of radezolid in lysosomes by proton trapping, as previously described for macrolides.

Antibiotic accumulation in phagocytic cells has been the subject of numerous studies over the last 20 years. These studies have examined to what extent drugs accumulate and where they distribute in cells and have also tried to address the mechanisms of entry and efflux. Several antibiotics have been profiled in this way, including beta-lactams, macrolides, fluoroquinolones, aminoglycosides, and glycolipopeptides (see references 2, 21, and 41 for recent key examples). Little is known so far, however, about oxazolidinones (30), although recent work showed that significant differences in accumulation can be observed between apparently closely related derivatives (19). Yet, oxazolidinones deserve special interest in this context, as they represent a useful alternative for treatment of infections caused by multidrug-resistant Gram-positive organisms, especially methicillin-resistant *Staphylococcus aureus* (MRSA) (46, 48), which we know to thrive and persist intracellularly (10, 23). Several new oxazolidinones are currently undergoing preclinical evaluation to assess potential improvements in activity and pharmacokinetic profile (see reference 44 for a review).

In the present study, we have focused our interest on radezolid (RX-1741), the first molecule brought to clinical evaluation in the subclass of biaryloxazolidinones (49, 50). Biaryloxazolidinones combine into a single molecular design the most important interactions defined by sparsomycin and linezolid with the 50S subunit of the ribosome. This confers to them an improved antimicrobial activity, including against linezolid-resistant strains (17, 35, 50). Within this family, radezolid was selected for further development and has shown appropriate efficacy and tolerability in ongoing phase 2 clinical trials for community-acquired pneumonia and uncomplicated skin and skin structure infections (12).

At the structural level, the presence of a secondary amine coupled with the triazole heterocycle confers to radezolid a dibasic character which markedly increases the ionization and hydrophilicity of the molecule at physiological pH. In contrast, linezolid can be considered a weak monobasic compound (Fig. 1 presents the chemical structure and Table 1 the pertinent physicochemical properties). These properties suggest potentially major differences in the way the two drugs could be processed by cells. This has triggered us to examine the cellular pharmacokinetics of radezolid in eukaryotic cells, using three types of phagocytes (human and murine macrophages and human polymorphonuclear neutrophils [PMN]). We provide a detailed description of uptake, subcellular distribution, and efflux and address the underlying mechanisms of these processes. Our studies use linezolid and azithromycin as comparator compounds. Azithromycin shares with radezolid an amphiphilic, dibasic character and is known to accumulate to high levels in phagocytic cells by a mechanism of diffusion through membranes and segregation in acidic compartments (6, 13). Although less extensively studied, linezolid is known to accumulate only modestly in cells (19).

Our studies show that radezolid accumulates about 11-fold

* Corresponding author. Mailing address: Unité de Pharmacologie cellulaire et moléculaire, Université catholique de Louvain, UCL 73.70, Avenue E. Mounier 73, B-1200 Brussels, Belgium. Phone: 3227647378. Fax: 3227647373. E-mail: francoise.vanbambeke@uclouvain.be.
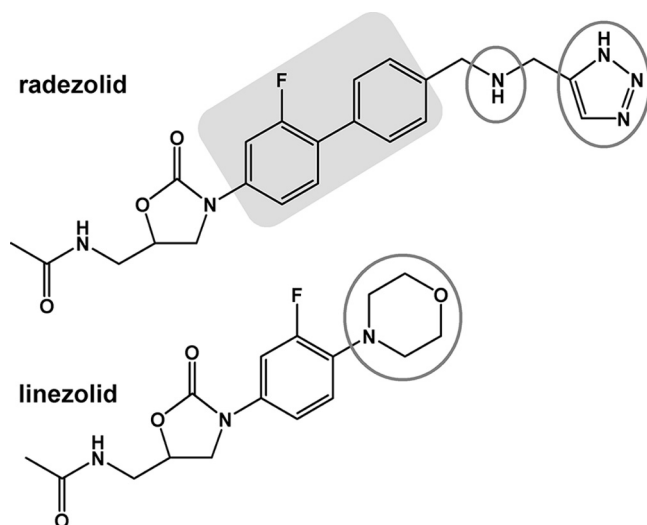
FIG. 1. Chemical structure and pertinent physicochemical properties of radezolid {*N*-[[(5S)-3-[2-fluoro-4′-[[(1H-1,2,3-triazol-5-yl-methyl)amino]methyl][1,1′-biphenyl]-4-yl]-2-oxo-5-oxazolidinyl]methyl] acetamide} and its parent compound linezolid. Gray circles show basic functions, and the light-gray box highlights the biaryl part of the molecule that is characteristic of the subfamily.

in phagocytic cells, with no evidence of active efflux. The accumulation is rapid and concentration and energy independent. In addition, radezolid displays a dual subcellular distribution, colocalizing to the cytosol and lysosomes with no specific association with mitochondria. These observations are compatible with a mechanism of diffusion/partial segregation in lysosomes by proton trapping.

(Parts of this study were presented at the 19th European Congress of Clinical Microbiology and Infectious Diseases, Helsinki, Finland, May 2009, as oral presentation O29, and at the 26th International Conference on Chemotherapy, Toronto, Ontario, Canada, June 2009, as an oral presentation.)

MATERIALS AND METHODS

Antibiotics and main reagents. Radezolid (RX-1741, supplied as microbiological standard powder with a potency of 93%) and [^{14}C]RX-1741 (25 mCi/mmol; labeled on the C of the methylacetamide replacing the oxazolidinone ring) were obtained from Rib-X Pharmaceuticals (New Haven, CT). [^{14}C]RX-1741 was diluted with the cold drug to obtain a stock solution at 1 mg/ml (4 μCi/ml) that was used for all experiments. Linezolid was obtained as the corresponding

branded product (Zyvoxid) distributed in Belgium for human use by Pfizer SA/NV (Brussels, Belgium), and azithromycin as the microbiological standard (potency of 94.4%) from Pfizer, Groton, CT. Verapamil, gemfibrozil, and monensin were purchased from Sigma-Aldrich (St. Louis, MO). Cell culture media and sera were from Invitrogen Corp. (Carlsbad, CA), and other reagents from Sigma-Aldrich or Merck KGaA (Darmstadt, Germany).

Cell lines. Most of the experiments were performed with 2 macrophage cell lines, namely, (i) human THP-1 cells (ATCC TIB-202 [American Tissue Culture Collection, Manassas, VA], a myelomonocytic cell line displaying macrophage-like activity [38]), and (ii) murine J774.1 cells (ATCC TIB-67). These cells were maintained in our laboratory as previously described (9, 27). Additional experiments were conducted with PMN, which were isolated from buffy coat samples obtained from healthy volunteers using the Histopaque (1007 and 1119; Sigma-Aldrich) gradient centrifugation technique (700 rpm, 30 min) (24). The purity of the preparation was estimated to be 85%, based on microscopic examination of cells stained with a Hemacolor staining kit (Merck KGaA, Darmstadt, Germany). The viability of the cells was checked by the trypan blue exclusion test and found to be >95%.

Accumulation and release experiments. Antibiotic accumulation and release were determined exactly as described earlier (32) for adherent cells, with adaptations for cells growing in suspension. In brief, cells incubated in the presence of antibiotics were washed three times in ice-cold phosphate-buffered saline (PBS) after suitable incubation times (THP-1 cells and PMN, which grow in suspension, were previously harvested by low-speed centrifugation). They were thereafter collected by centrifugation (THP-1 cells and PMN) or scraping (J774 cells) in distilled water. When measuring the kinetics of release, cells incubated with radezolid were washed, reincubated in a drug-free medium, and collected as described above. When studying the influence of extracellular pH, cells were incubated with buffered medium adjusted to specific pH values ranging from 5.0 to 7.4. The exact pH of each medium was measured before and after incubation and was found to not vary by more than 0.1 pH unit during the experiment.

Assay of cell-associated antibiotics. Cells lysates (obtained by sonication) were used for determination of antibiotic content and protein assay. Radezolid was assayed by liquid scintillation counting, cells having been incubated with the radiolabeled drug (lowest limit of detection, 0.003 mg/liter; linear response between 0.01 and 0.78 mg/liter; $R^2 = 0.999$). This method has been fully validated with respect to specificity, reproducibility, and linearity under the conditions of our assays. We also checked in pilot experiments that the antibiotic cell content measured by the disc plate method gave similar values (the *P* value was >0.4 when comparing concentrations determined by the two methods). Because the corresponding radiolabeled compounds were not available to us, linezolid and azithromycin were assayed by a microbiological method (disc plate assay), using *S. aureus* ATCC 25923 as test organism (linear response between 16 and 500 mg/liter [linezolid] and between 8 and 500 mg/liter [azithromycin]; R^2 values of 0.989 [linezolid] and 0.963 [azithromycin]). All cellular drug contents were expressed by reference to the total cell protein content (determined by the Lowry method) and converted into apparent total cell concentrations using a conversion factor of 5 μl per mg of cell protein (3).

Determination of protein binding in culture medium. The proportion of radezolid bound to serum proteins in our experimental conditions was evaluated after 2 h of incubation with [^{14}C]radezolid in culture medium containing increasing amounts of fetal calf serum. Bound and free fractions were separated using a Centrifree ultrafiltration device from Millipore (Carrigtwohill, Cork, Ireland) with a regenerated cellulose membrane (molecular mass cutoff, 30 kDa).

TABLE 1. Physicochemical properties of drugs

Drug	pK$_{a1}$[a]	pK$_{a2}$[a]	Calculated D/DH$^+$/DH$_2^{2+}$ ratio[b] at pH:		Calculated logP[c]	Calculated logD[d] (pH 7.4)
			7.4	5.4		
Linezolid	5.0		**71**/29/0	29/**71**/0	0.47	0.47
Radezolid	6.8	9.4	1/**79**/20	0/4/**96**	0.70	−1.40
Azithromycin	8.1	8.8	2/16/**82**	0/0/**100**	2.98	0.80

[a] The source of pK$_a$ values for linezolid was Steve Brickner, Pfizer (personal communication), for radezolid was Rib-X Pharmaceuticals, data on file (determined by cosolvent potentiometric titration), and for azithromycin was data communicated by Pfizer, Groton, CT.
[b] The nonionized drug (D)/monocation (DH$^+$)/dication (DH$_2^{2+}$) ratio was calculated as % DH$^+$ = 100/(1 + 10$^{pKa_1 - pH}$ + 10$^{pH - pKa_2}$); % DH$_2^{2+}$ = 100/(1 + 10$^{pH - pKa_1}$ + 10$^{2pH - pKa_1 - pKa_2}$); % D = 100 − DH$^+$ − DH$_2^{2+}$. A value in bold is the most abundant form for each drug at the pH considered.
[c] Partition coefficient (ratio of concentrations of un-ionized compound between octanol and water); calculated with QikProp (Schrödinger).
[d] Distribution coefficient (ratio of the sum of concentrations of all forms of the compound in each of these phases at pH 7.4); calculated as logP − log(1 + 10$^{pKa_2 - pH}$ + 10$^{pKa_1 + pKa_2 - 2pH}$) (16).
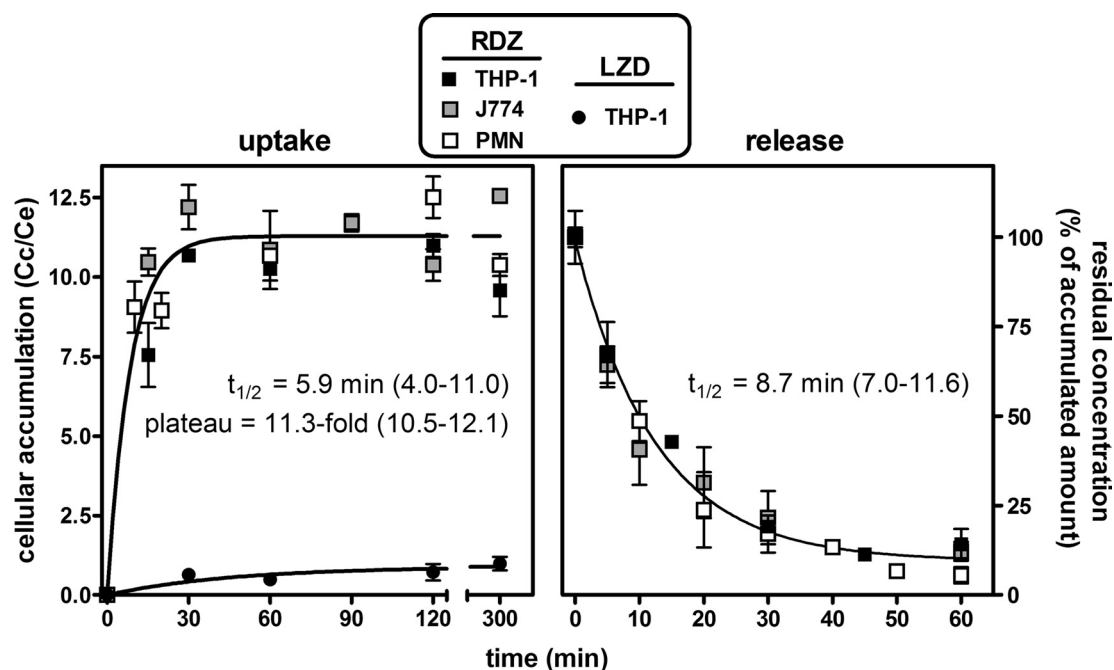
FIG. 2. Kinetics of radezolid uptake and release within THP-1 and J774 cell lines and PMNs. Left, uptake. Cells were incubated for up to 5 h in the presence of 4 mg/liter radezolid (RDZ) or 250 mg/liter linezolid (LZD). The ordinate shows the apparent cellular-to-extracellular concentration ratio. Data are fitted to one-phase exponential association ($R^2 = 0.837$ for RDZ, 0.824 for linezolid). Right, release. Cells were incubated with 4 mg/liter radezolid during 2 h before being transferred to drug-free medium. Values are expressed as the percentage of the accumulated amount at 2 h (time zero). Data are fitted to one-phase exponential decay ($R^2 = 0.988$). Results are given as means ± standard deviations ($n = 3$).

Amounts of 200 μl of samples were transferred to the ultrafiltration device and centrifuged for 10 min (2,000 × g, Eppendorf centrifuge 5810R equipped with an A-4-62 rotor) as previously described for linezolid (4). Radezolid was then quantified in the ultrafiltrate by scintillation counting; the bound concentration was calculated as the difference between the total concentration and the free concentration.

Cell fractionation studies of J774 cells. The major subcellular organelles were separated by combined differential and isopycnic centrifugations as previously described (42). In brief, cells were incubated with [^{14}C]radezolid for 2 h, washed free of antibiotics in 0.25 M sucrose, 1 mM EGTA, 3 mM imidazole (pH 7.4), and finally collected by gentle scraping in the same medium. The cells were then homogenized with a Dounce tissue grinder, and a cytoplasmic extract free of nuclei was obtained after three successive low-speed centrifugations (770, 625, and 500 × g, 10 min). The resulting cytoplasmic extract was further fractionated into a "granule" fraction (containing the bulk of the cells' organelles and membranes [MLP fraction]) and a final supernatant fraction (S fraction) by high-speed centrifugation (145,000 × g) for 30 min (Ti50 rotor; Beckman instruments, Inc., Fullerton, CA). The MLP fraction was further analyzed by isopycnic centrifugation in a linear sucrose gradient (10.9 ml, density limits 1.10 to 1.24, resting on a 600-μl 1.34 g/cm^3 cushion). After equilibration, 12 fractions of approximately 1 ml each were collected and weighed, and their densities were determined by refractometry. The amounts of protein and [^{14}C]radezolid were determined in each fraction in parallel with the activity of marker enzymes of the main organelles, namely, cytochrome c oxidase (for mitochondria), N-acetyl-β-glucosaminidase (for lysosomes), and lactate dehydrogenase (LDH; for cytosol). The results are expressed as the relative frequency of enzyme activity, protein, or drug recovered in each fraction as a function of the density of the fraction (standardized in sections of equal increments), the area of each histogram being equal to 1 (7, 32).

Assessment of cell viability. The viability of cells in the different experimental conditions (exposure to oxazolidinones [up to 50 mg/liter] or incubation in media at different pH, in the presence of monensin, or at low temperature) was evaluated by measuring the release of lactate dehydrogenase, which is a cytosolic enzyme (31), or the formation of purple formazan crystal dye [3-(4,5-dimethyl-thiazol-2-yl)-2,5-diphenyl tetrazolium bromide (MTT) assay (29)]. Using both

procedures, no significant differences (<10%) were detected between treated and control cells.

RESULTS

Cellular accumulation and release of radezolid in phagocytic cells. In a first series of experiments, we examined the kinetics of radezolid uptake and efflux in three types of phagocytic cells, namely, human macrophage-like THP-1 cells, murine J774 macrophages, and human PMN (Fig. 2). These experiments were performed with an extracellular concentration of radezolid of 4 mg/liter. In contrast to linezolid, which only reached a cellular concentration close to the extracellular one in THP-1 cells, radezolid accumulated quickly and markedly in these cells, reaching cellular levels ~12-fold higher than linezolid. The kinetics and extent of accumulation of radezolid seen with THP-1 cells was also observed with the other cell types investigated, with an accumulation half-life ($t_{1/2}$) of ~6 min and a maximal cellular-to-extracellular concentration ratio of ~11 (analysis of variance [ANOVA] of individual curves did not evidence any significant difference between cell types with respect to plateau values [$P = 0.957$] and accumulation constant rates [$k = 0.693/t_{1/2}$; $P = 0.252$]). Release was then examined in the three cell types after loading with radezolid for 2 h. The release rates ($k = 0.693/t_{1/2}$) were not significantly different ($P = 0.067$) between cell types, with a mean half-life of ~8.7 min.

Influence of radezolid's extracellular concentration and of serum concentration in the culture medium on cellular accumulation. We then examined the effect of increasing the ex-

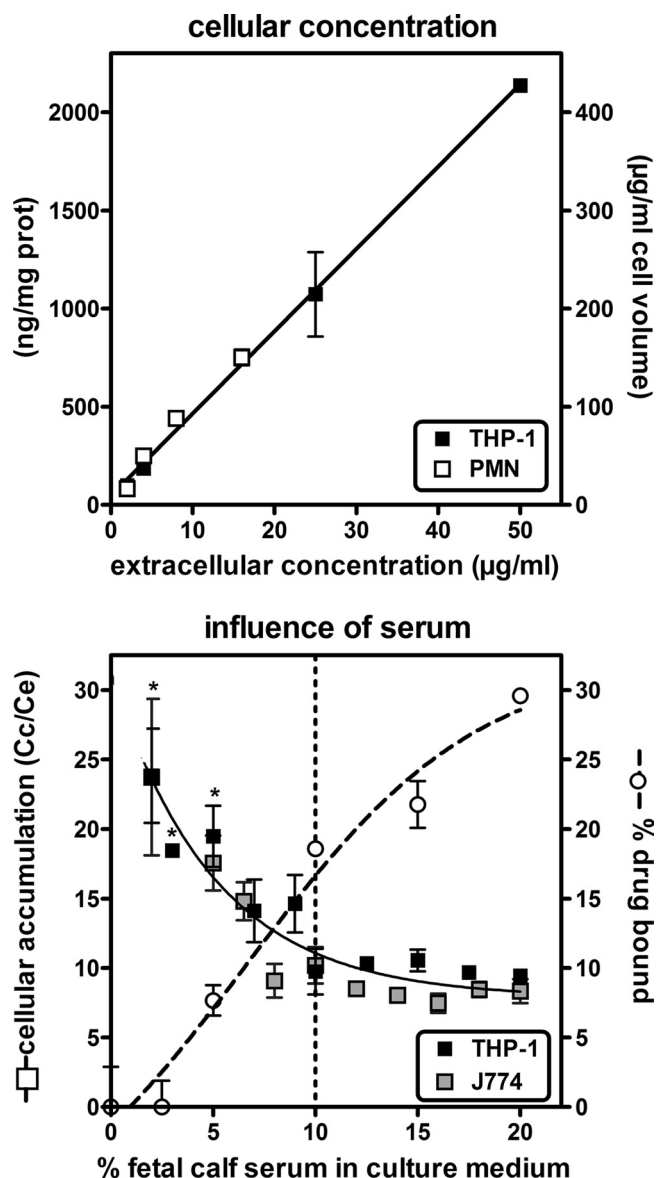## cellular concentration

influence of serum

FIG. 3. Upper panel, cellular concentration of radezolid in cells incubated for 2 h with increasing extracellular concentrations in medium supplemented with 10% fetal calf serum. Cellular concentrations are expressed either as ng/mg cell protein (prot) (left) or in µg/ml cell volume (conversion factor, 5 µl cell volume/mg of protein) (right). Data are fitted to a linear regression ($R^2 = 0.997$; slope, 8.5 for cellular concentration expressed in µg/ml cell volume, corresponding to the mean accumulation factor). Lower panel, influence of the fetal calf serum concentration in the culture medium on cellular accumulation of radezolid. Cells were incubated for 2 h with 4 mg/liter radezolid in medium supplemented with increasing concentrations of fetal calf serum. Left y axis, cellular accumulation factor of radezolid; right y axis, % radezolid bound to serum proteins. Data for cellular accumulation are fitted to one-phase exponential decay ($R^2 = 0.904$). A statistically significant difference ($P < 0.01$; one-way ANOVA with Dunnet multiple comparison test [comparison with 10% fetal calf serum]) is shown by an asterisk. Data for protein binding are fitted to sigmoidal regression ($R^2 = 0.974$). Results are given as means ± standard deviations ($n = 3$).

tracellular concentration on the accumulation of radezolid in 2-h uptake experiments (Fig. 3, upper panel). The cellular concentration increased linearly with no sign of saturation up to 50 mg/liter, with an apparent cellular-to-extracellular concentration ratio of approximately 8.5-fold over the entire range of extracellular concentrations investigated ($R^2 = 0.977$ for data pooled from THP-1 cells and PMN; there is no significant difference [t test] between linear regressions when data are plotted per cell line [$P = 0.438$]).

As the *in vitro* model used implies the presence of fetal bovine serum in the culture medium, we investigated whether its concentration would influence the capacity of radezolid to accumulate in cells. This was tested with human and murine macrophages incubated for 2 h with 4 mg/liter radezolid in medium supplemented with fetal calf serum from 2 to 20%, these limits being imposed by the maintenance of the viability of the cells. The data presented in Fig. 3 show that decreasing the serum concentration below the standard 10% caused a commensurate increase in radezolid accumulation, whereas increasing it above this value did not cause any significant decrease. The fraction of radezolid bound to serum proteins was determined in parallel for the culture medium; it increased from 0 to 28% when the content of serum was increased from 2.5% to 20%.

Mechanistic studies: influence of temperature, ATP-depletion, and efflux pump inhibitors. The next series of experiments was designed to achieve an understanding of the mechanisms involved in radezolid accumulation in cells, using THP-1 macrophages as a model (Fig. 4). All data were obtained after 2 h of incubation with 50 mg/liter radezolid, 250 mg/liter linezolid, or 10 mg/liter azithromycin. When cells were incubated at 4°C, the apparent cellular concentrations of radezolid and of linezolid decreased to about 35 to 40% of their control values (Fig. 4, left panel). In parallel experiments, we observed that radezolid's accumulation was not modified by either ATP depletion or efflux pump inhibitors, while that of azithromycin, a substrate of P-glycoprotein (34), was increased 1.7-fold in both situations (Fig. 4, middle and right panels). Additional experiments confirmed an absence of an effect of efflux pump inhibitors on (i) the rate of uptake and efflux of radezolid in THP-1 cells; (ii) its level of accumulation over a wide range of extracellular concentrations (4 to 50 mg/liter) in THP-1 cells; or (iii) its level of accumulation in J774 macrophages and PMN (data not shown).

Influence of the proton ionophore monensin and pH gradients. The dibasic character of radezolid (Fig. 1) suggests that pH gradients between cellular compartments and the ionization state of the molecule could play a determining role in its accumulation, as previously described for macrolides like azithromycin (13, 21). We therefore studied the effect of the proton ionophore monensin (known to dissipate transmembrane pH gradients) on radezolid accumulation in THP-1 cells, again in comparison with linezolid and azithromycin. We also tested how acidification of the extracellular medium or the combination of both conditions would affect these molecules. After incubating cells for 2 h in the presence of 50 µM monensin (Fig. 5, left panel), we observed marked reductions in the apparent cellular concentration of both oxazolidinones (residual value, 20% to 25% of control) and a still-larger reduction in that of azithromycin (residual value, 10% of control).
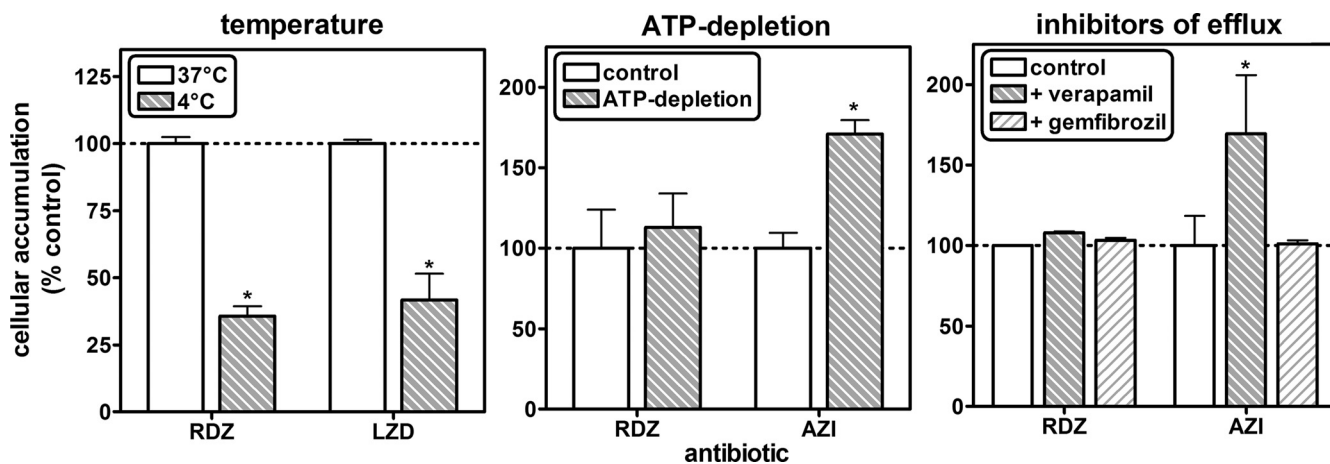
FIG. 4. Influence of temperature, ATP depletion, and efflux transporter inhibitors on radezolid accumulation in THP-1 cells (incubation time, 2 h; extracellular concentration of radezolid [RDZ] is 50 mg/liter, of linezolid [LZD] is 250 mg/liter, of azithromycin [AZI] is 10 mg/liter, of verapamil is 100 μM, and of gemfibrozil is 250 μM). ATP depletion was obtained by preconditioning cells during 1 h with 60 mM deoxyglucose and 5 mM NaN$_3$ and performing incubation in the same medium (27). The ordinate shows the apparent cellular-to-extracellular concentration ratio (% of control values). All results are given as means $\pm$ standard deviations ($n = 3$). A statistically significant difference ($P < 0.05$; t test in comparison with control) is shown by an asterisk.

Likewise, acidification of the culture medium (Fig. 5, middle panel) caused progressive decreases in the apparent cellular concentration of both oxazolidinones at 30 min when the pH of the culture medium was reduced from 7.0 to 6.0, to reach again 25% of control values for a pH value of ≤6.0.

The azithromycin accumulation fell to 10% of control values as soon as the pH was brought from 7.0 to ≤6.5. Interestingly enough, monensin did not affect radezolid's accumulation in cells incubated in medium adjusted at a pH value of <7.0 but caused a significant decrease at a pH value of ≥7.0, with the residual accumulation remaining similar to that measured in the absence of monensin at pH 6.5 (Fig. 5, right panel). The same experiments were performed with J774 cells, with similar

results (residual accumulation, 30% of control values in the presence of monensin or at pH 5; data not shown).

Subcellular localization of radezolid in J774 macrophages. These studies were performed with J774 cells because preliminary experiments with THP-1 cells, using both sucrose and Percoll gradients, showed that the distribution of lysosomes and of mitochondria could not be satisfactorily resolved in these cells based on density equilibration. We first separated cell homogenates into an unbroken cell/nucleus fraction and a cytoplasmic extract using low-speed centrifugation. The unbroken cells and nuclei contained about 20% of the total activity of each enzymatic marker (lactate dehydrogenase, N-acetyl-β-glucosaminidase, and cytochrome c oxidase) and about 20% of
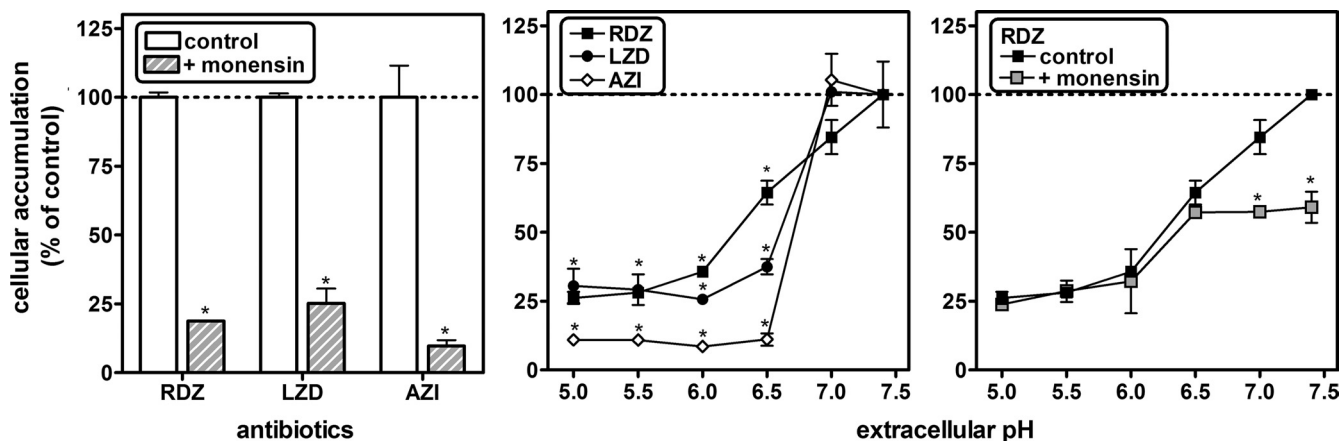
FIG. 5. Influence of the proton ionophore monensin and of extracellular pH on radezolid, linezolid, and azithromycin accumulation in THP-1 macrophages (extracellular concentration of radezolid [RDZ] is 50 mg/liter, of linezolid [LZD] is 250 mg/liter, and of azithromycin [AZI] is 10 mg/liter). Left, cells coincubated with 50 μM monensin during 2 h; middle, cells incubated in pH-adjusted medium during 30 min; right, cells coincubated with 50 μM monensin in pH-adjusted medium during 30 min. The ordinate shows the apparent cellular-to-extracellular concentration ratio (% of control values [no monensin or pH 7.4]). All results are given as means $\pm$ standard deviations ($n = 3$). A statistically significant difference ($P < 0.01$; Student's t test [left and right panels, comparison of control with monensin-treated cells] or one-way ANOVA with Dunnet multiple comparison test [middle panel, comparison with pH 7.4]) is shown by an asterisk.
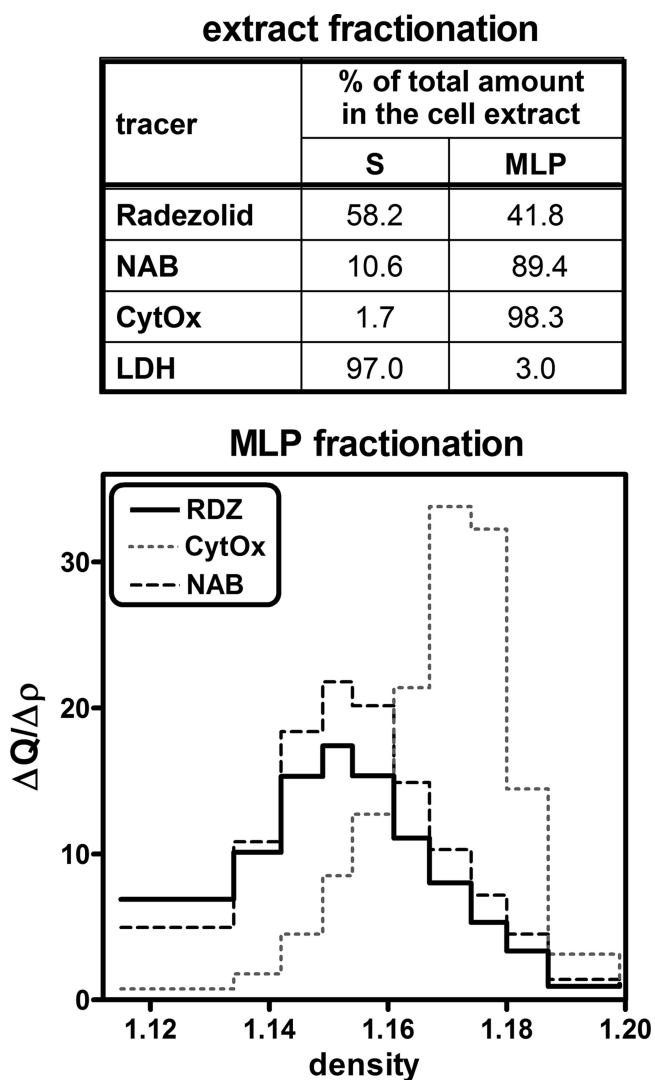
extract fractionation

tracer	% of total amount in the cell extract	
	S	**MLP**
Radezolid	58.2	41.8
NAB	10.6	89.4
CytOx	1.7	98.3
LDH	97.0	3.0

MLP fractionation

FIG. 6. Distribution of marker enzymes (N-acetyl-β-glucosaminidase [NAB; lysosomes], cytochrome c oxidase [CytOx; mitochondria], and lactate dehydrogenase [LDH; cytosol]) and radezolid [RDZ] upon fractionation of J774 cells incubated during 2 h in the presence of 50 mg/liter of [^{14}C]radezolid. The upper panel (extract fractionation) summarizes the percentage of each constituent recovered in supernatant (S) or granular (MLP) fractions. The lower panel shows the density distribution of each constituent within the MLP fraction in a linear sucrose gradient. y axis, relative frequency (fractional quantity in each fraction/density increment).

the radezolid-associated radioactivity (data not shown). As we see the same percentage for all markers in this fraction, this suggests no specific association of radezolid to nuclei. The cytoplasmic fraction was then further separated by high-speed centrifugation into a supernatant (S) and a granular fraction (MLP) containing the bulk of the mitochondria, lysosomes, and endoplasmic reticulum. About 42% of the cell-associated radezolid was recovered in the granular fraction (MLP), while 58% was recovered in the supernatant (S) (Fig. 6, upper panel). As expected, lactate dehydrogenase activity was almost exclusively recovered in the supernatant, while 90% of the N-acetyl-β-glucosaminidase and 98% of the cytochrome c ox-

idase activities were found in the MLP. The MLP fraction was then further fractionated by isopycnic centrifugation to establish the distribution of radezolid between the organelles present in this fraction (Fig. 6, lower panel). The distribution of radezolid could be superimposed on that of the lysosomal marker (N-acetyl-β-glucosaminidase) and was clearly distinct from that of the mitochondrial marker (cytochrome c oxidase), with modal equilibration densities of 1.15 and 1.17, respectively.

DISCUSSION

The data presented in this paper show that radezolid accumulates intracellularly to about 10- to 12-fold its extracellular levels in three types of phagocytic cells. This process is rapid, reversible, nonsaturable, and energy independent but pH dependent. It drives the drug to the cytosolic and lysosomal compartments. This level of accumulation contrasts with that of linezolid, for which we found an accumulation factor close to 1. This is consistent with in vivo data describing linezolid as an antibiotic with high diffusibility in body tissues but poor cellular accumulation, reaching, in human alveolar macrophages, a concentration lower than in serum (14).

To further probe the mechanism(s) involved in radezolid uptake, we first examined influx and efflux mechanisms. Our data are compatible with a passive diffusion process, and this is for four main reasons. First, the rate of uptake and efflux is similar and quite fast in all cell types investigated, with an apparent half-life of 6 to 10 min. These rates are of the same order of magnitude for drugs known to enter cells by diffusion, such as macrolides (8, 13), fluoroquinolones (7, 27), or chloroquine (42). These rates are, however, much faster than those observed for antibiotics accumulating by fluid-phase pinocytosis, such as aminoglycosides in nonrenal cells (39) or oritavancin in macrophages (42). Furthermore, the involvement of a cell-specific transport system is unlikely because (i) the rates of uptake and levels of accumulation of radezolid are quite similar in the three cell types investigated (as well as several types of nonphagocytic cells; see our companion paper [18]) and (ii) its accumulation is nonsaturable over a wide range of extracellular concentrations, as previously described for azithromycin (13). Second, the accumulation of radezolid is not modified by ATP depletion but is markedly reduced by incubating the cells at 4°C. The first observation rules out a potential active intake process, and the second one, also described with azithromycin (13), highlights the importance of membrane fluidity for drug diffusion, as is generally known in most in vitro and in vivo systems (see reference 25 for a review). These data, as well as the absence of effect of efflux pump inhibitors on radezolid accumulation, also suggest that this drug is not subject to active efflux by those multidrug resistance proteins known to decrease the intracellular accumulation of fluoroquinolones (MRP [27]) or macrolides and daptomycin (P-glycoprotein) (20, 34). Third, the higher accumulation of radezolid measured in medium with low serum content suggests that only the free fraction is able to enter the cells, which is what one would expect from a diffusible drug. The plateau of accumulation reached at a higher serum content may reflect a displacement of the protein-bound fraction as the free drug enters the cell. This suggests that a dynamic equilibrium between intracellular

and extracellular compartments may take place, with the predominant flux oriented toward the cells as described for azithromycin (33). Finally, it must be emphasized that both the logP and logD values of radezolid are in the range of those considered compatible with drug membrane permeability (5, 22). Also of interest, azithromycin and radezolid display similar logD values calculated at pH 7.4 (Table 1), suggesting comparable capacity to cross the pericellular membrane.

Moving now to the mechanism of accumulation itself, our data are highly suggestive of a proton-driven segregation of radezolid in acidic compartments, somewhat following the model described to explain the cellular accumulation of weakly basic drugs in cells (45) and in lysosomes (11) and best illustrated by macrolides in the field of antiinfective pharmacology (6, 8). We show here that radezolid indeed displays a dual localization, with about 60% recovered in the soluble fraction and 40% distributing together with a lysosomal enzyme in the large-organelle fraction. This means a moderate accumulation in the cytosol (about 6-fold) but a much larger one in the lysosomes (about 80-fold or higher, based on a lysosomal volume of 5% or less than the total cell volume, as estimated in macrophages or fibroblasts [1, 36]). These data may actually reflect the gradients of pH between the extracellular milieu and the cytosol (about 0.4 pH units) or the lysosomes (about 2 pH units), respectively. This is also consistent with our observation of a marked decrease in cellular accumulation at acidic pH (which will reduce the pH gradient between medium and cytosol and lysosomes) and in the presence of monensin (known to collapse the cytosol-lysosomal pH gradient [37]). This is quite similar to what was observed for azithromycin (6, 40). For radezolid, however, the proportion of the drug found in the lysosomes is lower than that reported for azithromycin (40% versus 50 to 70% [6]) and the residual accumulation in the presence of monensin or at acidic pH remains higher than for azithromycin. This probably results from differences in pK_a values (Table 1), with azithromycin being more basic and therefore more fully protonated at acidic pH than radezolid. Of interest also, cellular fractionation studies did not show any specific association of radezolid with mitochondria, which are the target organelle for oxazolidinone and chloramphenicol toxicity (26, 47).

The unavailability of radiolabeled linezolid prevented us from performing as detailed experiments with this drug as we were able to do with radezolid, especially with respect to kinetics of uptake and efflux and determination of subcellular distribution. Yet, we observed a globally similar effect of monensin and of acidification of the culture medium on linezolid's accumulation. Actually, the differences in accumulation levels observed between linezolid, radezolid, and azithromycin can easily be explained by commensurate differences in the relative abundances of their charged and uncharged species on the one hand and their lipophilicity (as illustrated by logP and logD values) on the other hand. The model of proton-driven segregation of weak basic drugs in membrane-bounded compartments implies, indeed, that accumulation at equilibrium will be directly proportional (i) to the ratio of the permeability constants of the nonionized to the ionized forms of the molecules and (ii) to the number and the pK_a of the basic ionizable functions. Based on what is known about those properties, this clearly rationalizes the ranking in accumulation observed here

(namely, linezolid < radezolid < azithromycin), as well as the fact that extracellular pH modulates radezolid's accumulation over a 1-unit range (7.0 to 6.0) instead of the 0.5-unit range (7.0 to 6.5) for azithromycin. For azithromycin, its capacity to bind to negatively charged phospholipids may further enhance its accumulation (28, 43). Of note also, the cellular accumulation of radezolid was not influenced by a variation of pH from 7.4 to 6.5 in the extracellular milieu when monensin was present (Fig. 5, right panel). This is consistent with the facts that (i) monensin acts specifically on the ATP-driven pump responsible for acidifying lysosomes (37) to values as low as pH 5.5 and does not appear affect the cytosol's pH (which is around 7) and (ii) the pK_{a1} of radezolid is close to this value, making it a turning point for a significant change in the ratio of the monocationic and dicationic forms of the drug.

We recently observed that another oxazolidinone, torezolid (TR700), shows a larger cellular accumulation than linezolid and a greater-than-90% reduction in uptake upon acidification of the culture medium (19). Direct comparison with the radezolid cellular pharmacokinetics described here, however, cannot be made, as (i) we do not know torezolid's subcellular localization and (ii) torezolid's physicochemical properties are quite distinct from those of radezolid (torezolid being not a dicationic drug but being slightly more lipophilic than linezolid, about 0.4 log units for both logP and logD, calculated using QikProp software [Schrõdinger, LLC, Portland, OR]).

Although still far from reproducing the situation prevailing *in vivo*, the design of our experiments has allowed us to address the impact of protein binding on drug handling by cells. We first see that increasing the protein content above its standard value does not change the level of accumulation of radezolid at equilibrium. We also show that radezolid's accumulation is similar in various cell lines, in freshly isolated human PMNs, and in primary cultures of human keratinocytes (see also the companion paper [18]), suggesting that what we describe is a general property of this drug.

Besides their interest for the knowledge of pharmacological properties of radezolid and other oxazolidinones, our findings may have important clinical implications. First, the fact that radezolid accumulates to higher levels than linezolid may explain its larger volume of distribution (V), as animal data indicate for radezolid a V 1.5- to 1.8-fold higher than that of linezolid in mice, rats, or dogs (see reference 15 and Rib-X data on file). This may help the drug achieve improved tissue penetration and a higher concentration in the infected compartment. High concentration in PMNs may also contribute to the conveyance and delivery of the drug at the site of infection, as previously proposed for azithromycin (33).

Second, although the correlation is extremely variable from one antibiotic class to another, a higher cellular concentration may help the antibiotic to exert useful activity against intracellular bacteria (see reference 41 for a review). This issue is examined in detail in the companion paper (18).

REFERENCES

1. **Aubert-Tulkens, G., F. Van Hoof, and P. Tulkens.** 1979. Gentamicin-induced lysosomal phospholipidosis in cultured rat fibroblasts. Quantitative ultrastructural and biochemical study. Lab. Invest. **40:**481–491.

2. **Barcia-Macay, M., F. Mouaden, M. P. Mingeot-Leclercq, P. M. Tulkens, and F. Van Bambeke.** 2008. Cellular pharmacokinetics of telavancin, a novel lipoglycopeptide antibiotic, and analysis of lysosomal changes in cultured eukaryotic cells (J774 mouse macrophages and rat embryonic fibroblasts). J. Antimicrob. Chemother. **61:**1288–1294.

3. **Barcia-Macay, M., C. Seral, M. P. Mingeot-Leclercq, P. M. Tulkens, and F. Van Bambeke.** 2006. Pharmacodynamic evaluation of the intracellular activities of antibiotics against Staphylococcus aureus in a model of THP-1 macrophages. Antimicrob. Agents Chemother. **50:**841–851.

4. **Buerger, C., N. Plock, P. Dehghanyar, and C. Kloft.** 2006. Pharmacokinetics of unbound linezolid in plasma and tissue interstitium of critically ill patients after multiple dosing using microdialysis. Antimicrob. Agents Chemother. **50:**2455–2463.

5. **Camenisch, G., J. Alsenz, H. van de Waterbeemd, and G. Folkers.** 1998. Estimation of permeability by passive diffusion through Caco-2 cell monolayers using the drugs' lipophilicity and molecular weight. Eur. J. Pharm. Sci. **6:**317–324.

6. **Carlier, M. B., I. Garcia-Luque, J. P. Montenez, P. M. Tulkens, and J. Piret.** 1994. Accumulation, release and subcellular localization of azithromycin in phagocytic and non-phagocytic cells in culture. Int. J. Tissue React. **16:**211–220.

7. **Carlier, M. B., B. Scorneaux, A. Zenebergh, J. F. Desnottes, and P. M. Tulkens.** 1990. Cellular uptake, localization and activity of fluoroquinolones in uninfected and infected macrophages. J. Antimicrob. Chemother. **26**(Suppl. B):27–39.

8. **Carlier, M. B., A. Zenebergh, and P. M. Tulkens.** 1987. Cellular uptake and subcellular distribution of roxithromycin and erythromycin in phagocytic cells. J. Antimicrob. Chemother. **20**(Suppl. B):47–56.

9. **Carryn, S., S. Van de Velde, F. Van Bambeke, M. P. Mingeot-Leclercq, and P. M. Tulkens.** 2004. Impairment of growth of Listeria monocytogenes in THP-1 macrophages by granulocyte macrophage colony-stimulating factor: release of tumor necrosis factor-alpha and nitric oxide. J. Infect. Dis. **189:**2101–2109.

10. **Clement, S., P. Vaudaux, P. Francois, J. Schrenzel, E. Huggler, S. Kampf, C. Chaponnier, D. Lew, and J. S. Lacroix.** 2005. Evidence of an intracellular reservoir in the nasal mucosa of patients with recurrent Staphylococcus aureus rhinosinusitis. J. Infect. Dis. **192:**1023–1028.

11. **de Duve, C., T. de Barsy, B. Poole, A. Trouet, P. Tulkens, and F. Van Hoof.** 1974. Commentary. Lysosomotropic agents. Biochem. Pharmacol. **23:**2495–2531.

12. **File, T., Jr., F. Bagheri, L. Bush, J. Desanto, A. Markowitz, J. Pullman, R. Topkis, E. Burak, and S. Hopkins.** 2008. A phase 2 study comparing two doses of radezolid to linezolid in adults with uncomplicated skin and skin structure infections (uSSSI), poster L-1515c. Abstr. 48th Annu. Intersci. Conf. Antimicrob. Agents Chemother. (ICAAC)-Infect. Dis. Soc. Am. (IDSA) 46th Annu. Meet. American Society for Microbiology and Infectious Diseases Society of America, Washington, DC.

13. **Gladue, R. P., and M. E. Snider.** 1990. Intracellular accumulation of azithromycin by cultured human fibroblasts. Antimicrob. Agents Chemother. **34:**1056–1060.

14. **Honeybourne, D., C. Tobin, G. Jevons, J. Andrews, and R. Wise.** 2003. Intrapulmonary penetration of linezolid. J. Antimicrob. Chemother. **51:**1431–1434.

15. **Jing, H., X. Luo, K. Harrington, J. Sutcliffe, and E. Burak.** 2005. The pharmacokinetics of designer oxazolidinones in Sprague-Dawley rats, poster F-1261. 45th Intersci. Conf. Antimicrob. Agents Chemother. American Society for Microbiology, Washington, DC.

16. **Kallinteri, P., and S. G. Antimisiaris.** 2001. Solubility of drugs in the presence of gelatin: effect of drug lipophilicity and degree of ionization. Int. J. Pharm. **221:**219–226.

17. **Lawrence, L., P. Danese, J. DeVito, F. Franceschi, and J. Sutcliffe.** 2008. In vitro activities of the Rx-01 oxazolidinones against hospital and community pathogens. Antimicrob. Agents Chemother. **52:**1653–1662.

18. **Lemaire, S., K. Kosowska-Shick, P. C. Appelbaum, G. Verween, P. M. Tulkens, and F. Van Bambeke.** 2010. Cellular pharmacodynamics of the novel biaryloxazolidinone radezolid: studies with infected phagocytic and non-phagocytic cells, using *Staphylococcus aureus*, *Staphylococcus epidermidis*, *Listeria monocytogenes*, and *Legionella pneumophila*. Antimicrob. Agents Chemother. **54:**2549–2559.

19. **Lemaire, S., F. Van Bambeke, P. C. Appelbaum, and P. M. Tulkens.** 2009.

20. **Lemaire, S., F. Van Bambeke, M. P. Mingeot-Leclercq, and P. M. Tulkens.** 2007. Modulation of the cellular accumulation and intracellular activity of daptomycin towards phagocytized Staphylococcus aureus by the P-glycoprotein (MDR1) efflux transporter in human THP-1 macrophages and Madin-Darby canine kidney cells. Antimicrob. Agents Chemother. **51:**2748–2757.

21. **Lemaire, S., F. Van Bambeke, and P. M. Tulkens.** 2009. Cellular accumulation and pharmacodynamic evaluation of the intracellular activity of CEM-101, a novel fluoroketolide, against Staphylococcus aureus, Listeria monocytogenes, and Legionella pneumophila in human THP-1 macrophages. Antimicrob. Agents Chemother. **53:**3734–3743.

22. **Lipinski, C. A., F. Lombardo, B. W. Dominy, and P. J. Feeney.** 2001. Experimental and computational approaches to estimate solubility and permeability in drug discovery and development settings. Adv. Drug Deliv. Rev. **46:**3–26.

23. **Lowy, F. D.** 2000. Is Staphylococcus aureus an intracellular pathogen? Trends Microbiol. **8:**341–343.

24. **Luo, Y., and M. E. Dorf.** 1997. Isolation of mouse neutrophils. Curr. Protoc. Immunol. **3:**20.1-20.6.

25. **Martinez, M. N., and G. L. Amidon.** 2002. A mechanistic approach to understanding the factors affecting drug absorption: a review of fundamentals. J. Clin. Pharmacol. **42:**620–643.

26. **McKee, E. E., M. Ferguson, A. T. Bentley, and T. A. Marks.** 2006. Inhibition of mammalian mitochondrial protein synthesis by oxazolidinones. Antimicrob. Agents Chemother. **50:**2042–2049.

27. **Michot, J. M., F. Van Bambeke, M. P. Mingeot-Leclercq, and P. M. Tulkens.** 2004. Active efflux of ciprofloxacin from J774 macrophages through an MRP-like transporter. Antimicrob. Agents Chemother. **48:**2673–2682.

28. **Montenez, J. P., F. Van Bambeke, J. Piret, A. Schanck, R. Brasseur, P. M. Tulkens, and M. P. Mingeot-Leclercq.** 1996. Interaction of the macrolide azithromycin with phospholipids. II. Biophysical and computer-aided conformational studies. Eur. J. Pharmacol. **314:**215–227.

29. **Morgan, D. M.** 1998. Tetrazolium (MTT) assay for cellular viability and activity. Methods Mol. Biol. **79:**179–183.

30. **Pascual, A., S. Ballesta, I. Garcia, and E. J. Perea.** 2002. Uptake and intracellular activity of linezolid in human phagocytes and nonphagocytic cells. Antimicrob. Agents Chemother. **46:**4013–4015.

31. **Racher, A. J., D. Looby, and J. B. Griffiths.** 1990. Use of lactate dehydrogenase release to assess changes in culture viability. Cytotechnology **3:**301–307.

32. **Renard, C., H. J. Vanderhaeghe, P. J. Claes, A. Zenebergh, and P. M. Tulkens.** 1987. Influence of conversion of penicillin G into a basic derivative on its accumulation and subcellular localization in cultured macrophages. Antimicrob. Agents Chemother. **31:**410–416.

33. **Schentag, J. J., and C. H. Ballow.** 1991. Tissue-directed pharmacokinetics. Am. J. Med. **91:**5S–11S.

34. **Seral, C., J. M. Michot, H. Chanteux, M. P. Mingeot-Leclercq, P. M. Tulkens, and F. Van Bambeke.** 2003. Influence of P-glycoprotein inhibitors on accumulation of macrolides in J774 murine macrophages. Antimicrob. Agents Chemother. **47:**1047–1051.

35. **Skripkin, E., T. S. McConnell, J. DeVito, L. Lawrence, J. A. Ippolito, E. M. Duffy, J. Sutcliffe, and F. Franceschi.** 2008. R chi-01, a new family of oxazolidinones that overcome ribosome-based linezolid resistance. Antimicrob. Agents Chemother. **52:**3550–3557.

36. **Steinman, R. M., S. E. Brodie, and Z. A. Cohn.** 1976. Membrane flow during pinocytosis. A stereologic analysis. J. Cell Biol. **68:**665–687.

37. **Tartakoff, A. M.** 1983. Perturbation of vesicular traffic with the carboxylic ionophore monensin. Cell **32:**1026–1028.

38. **Tsuchiya, S., M. Yamabe, Y. Yamaguchi, Y. Kobayashi, T. Konno, and K. Tada.** 1980. Establishment and characterization of a human acute monocytic leukemia cell line (THP-1). Int. J. Cancer. **26:**171–176.

39. **Tulkens, P. M., and A. Trouet.** 1978. The uptake and intracellular accumulation of aminoglycoside antibiotics in lysosomes of cultured rat fibroblasts. Biochem. Pharmacol. **27:**415–424.

40. **Tyteca, D., P. Van Der Smissen, F. Van Bambeke, K. Leys, P. M. Tulkens, P. J. Courtoy, and M. P. Mingeot-Leclercq.** 2001. Azithromycin, a lysosomotropic antibiotic, impairs fluid-phase pinocytosis in cultured fibroblasts. Eur. J. Cell Biol. **80:**466–478.

41. **Van Bambeke, F., M. Barcia-Macay, S. Lemaire, and P. M. Tulkens.** 2006. Cellular pharmacodynamics and pharmacokinetics of antibiotics: current views and perspectives. Curr. Opin. Drug Discov. Devel. **9:**218–230.

42. **Van Bambeke, F., S. Carryn, C. Seral, H. Chanteux, D. Tyteca, M. P. Mingeot-Leclercq, and P. M. Tulkens.** 2004. Cellular pharmacokinetics and pharmacodynamics of the glycopeptide antibiotic oritavancin (LY333328) in a model of J774 mouse macrophages. Antimicrob. Agents Chemother. **48:**2853–2860.

43. **Van Bambeke, F., J. P. Montenez, J. Piret, P. M. Tulkens, P. J. Courtoy, and M. P. Mingeot-Leclercq.** 1996. Interaction of the macrolide azithromycin

with phospholipids. I. Inhibition of lysosomal phospholipase A1 activity. Eur. J. Pharmacol. **314:**203–214.

44. **Vara Prasad, J. V.** 2007. New oxazolidinones. Curr. Opin. Microbiol. **10:** 454–460.

45. **Waddell, W. J., and R. G. Bates.** 1969. Intracellular pH. Physiol. Rev. **49:** 285–329.

46. **Wilcox, M. H.** 2005. Update on linezolid: the first oxazolidinone antibiotic. Expert Opin. Pharmacother. **6:**2315–2326.

47. **Yunis, A. A., U. S. Smith, and A. Restrepo.** 1970. Reversible bone marrow suppression from chloramphenicol. A consequence of mitochondrial injury. Arch. Intern. Med. **126:**272–275.

48. **Zhanel, G. G., C. Shroeder, L. Vercaigne, S. Gin, J. Embil, and J. Hoban.** 2001. A critical review of oxazolidinones: an alternative or replacement for glycopeptides and streptogramins? Can. J. Infect. Dis. **12:**379–390.

49. **Zhou, J., A. Bhattacharjee, S. Chen, Y. Chen, E. Duffy, J. Farmer, J. Goldberg, R. Hanselmann, J. A. Ippolito, R. Lou, A. Orbin, A. Oyelere, J. Salvino, D. Springer, J. Tran, D. Wang, Y. Wu, and G. Johnson.** 2008. Design at the atomic level: design of biaryloxazolidinones as potent orally active antibiotics. Bioorg. Med. Chem. Lett. **18:**6175–6178.

50. **Zhou, J., A. Bhattacharjee, S. Chen, Y. Chen, E. Duffy, J. Farmer, J. Goldberg, R. Hanselmann, J. A. Ippolito, R. Lou, A. Orbin, A. Oyelere, J. Salvino, D. Springer, J. Tran, D. Wang, Y. Wu, and G. Johnson.** 2008. Design at the atomic level: generation of novel hybrid biaryloxazolidinones as promising new antibiotics. Bioorg. Med. Chem. Lett. **18:**6179–6183.